Green Chemistry

Efficient Transfer Hydrogenation of Carbonate Salts from Glycerol using Water-Soluble Iridium N-Heterocyclic Carbene Catalysts

Journal:	*Green Chemistry*
Manuscript ID	GC-ART-06-2020-001958.R2
Article Type:	Paper
Date Submitted by the Author:	25-Jul-2020
Complete List of Authors:	Ainembabazi, Diana; George Washington University, Chemistry Wang, Kai; George Washington University, Chemistry Finn, Matthew; George Washington University, Department of Chemistry Ridenour, James; George Washington University, Chemistry Voutchkova, Adelina; George Washington University, Chemistry

ARTICLE

Efficient Transfer Hydrogenation of Carbonate Salts from Glycerol using Water-Soluble Iridium N-Heterocyclic Carbene Catalysts

Received 00th January 20xx,
Accepted 00th January 20xx

DOI: 10.1039/x0xx00000x

Diana Ainembabazi[a], Kai Wang[a], Matthew Finn[a], James Ridenour[a], Adelina Voutchkova-Kostal[a*]

The transfer hydrogenation of CO_2 and carbonates from biomass-derived alcohols, such as glycerol, to afford formic and lactic acid is a highly attractive path to valorizing two waste streams, and is significantly more thermodynamically favorable than direct carbonate hydrogenation. Expanding on our seminal report of the first homogeneous catalyst for this process, here we show that thermally-robust and water-soluble Ir(I) and Ir(III) N-heterocyclic carbene (NHC) complexes with sulfonate-functionalized wingtips are highly prolific and robust catalysts for carbonate transfer hydrogenation from glycerol, requiring no additives in aqueous media. The most prolific catalyst of the nine examined, [Ir(NHC-Ph-SO_3^-)$_2CO_2$]Na (cat ***7***), effectively facilitates the reaction at low catalyst loading (10 ppm) at 150 °C using microwave or conventional heating. The cation of the carbonate salt significantly impacts catalytic activity, with highest activity observed with Cs_2CO_3 (27850 and 13350 TONs for lactate and formate respectively in 6 hours, compared to 15400 and 8120 with K_2CO_3). Catalytic amounts of Cs^+ were found to significantly enhance activity with K_2CO_3. Catalyst ***7*** is even more prolific with conventional heating under a positive N_2 pressure, reaching TOFs of >3000 h^{-1} and >2100 h^{-1} respectively for lactate and formate with K_2CO_3. The high activity of this catalyst compared to non-sulfonated and cyclooctadiene analogs is attributed to a combination of catalyst solubility in aqueous media and presence of π-acceptor carbonyl ligands. A catalytic mechanism is proposed for ***7*** involving O-H oxidative addition of glycerol, β-hydride elimination, bicarbonate dehydroxylation, insertion and reductive elimination.

Introduction

The development of methods to convert CO_2 and carbonates to valuable chemicals, such as formic acid, formaldehyde and methanol, has attracted increased interest due to the abundance of this C1 feedstock. Formic acid is a particularly valuable target, given the recent increase in its demand for applications ranging from chemical feedstocks,[1] fuels,[2] hydrogen storage media,[3] as well as commodity chemicals for food and agriculture.[1] The primary synthetic route to formic acid form CO_2 is direct hydrogenation, which since its first report in the 70's[4] continues to be an active area of research. Among the most active homogeneous catalysts reported for CO_2 hydrogenation are Rh,[5, 6] Ru,[7, 8] Ir,[9] Fe,[10] Ni[11] and Co.[12] However, direct hydrogenation of CO_2 is a thermodynamically unfavourable process (ΔG = 13.4 kcal/mol),[24] requiring base, amine additives and/or aqueous conditions to drive the reaction by stabilizing the product as the formate salt.[8, 13, 14] Given that in basic aqueous media CO_2 is in equilibrium with HCO_3^- (pK_{a1} = 6.35), the species undergoing hydrogenation could be either bicarbonate or carbonate.[8] Explicit hydrogenation of bicarbonate has been shown with Rh,[6, 15, 16] Ru,[17, 18, 19] Ir,[20] and Fe[21] catalysts. The thermodynamic driving force of bicarbonate hydrogenation in aqueous media is greater than that of CO_2 ($\Delta G°_{aq}$ = 4.4 kcal/mol for HCO_3^- vs 13.4 kcal/mol for CO_2,[22] consistent with trends reported by Papai et al[23]). Despite that, reported catalytic activities for carbonates are generally lower than those for CO_2 (maximum TOF reported is 551 hr^{-1} for bicarbonate,[18] vs > 23,000 hr^{-1} for CO_2).[24] ESI Scheme S1 summarizes the efficiency of recent catalytic examples for direct hydrogenation of both substrates.

Given that commercial H_2 gas is most commonly produced by steam reforming of natural gas, the use of renewable sources of hydrogen using transfer hydrogenation (TH) strategies is highly desirable form a sustainability perspective, as long as high selectivity and activity can be achieved. TH strategies also have process advantages relative to direct hydrogenation, such as the use of milder reaction conditions, elimination of use of flammable hydrogen, and ability to produce secondary products of commercial value. The generation of such by-products has the potential to improve the economics of the overall process, provided the by-product is more valuable than the hydrogen donor used, and is formed selectively.

Recently, we highlighted another key advantage of transfer hydrogenation (TH) of CO_2 vs direct hydrogenation: overcoming the unfavourable thermodynamics of the latter.[22] The thermodynamics of the TH process strongly depend on choice of H-donor under basic conditions: isopropanol, for example, lowers ΔG by 9.7 kcal/mol vs direct hydrogenation of CO_2, while glycerol lowers it by 22.6 kcal/mol. The significant driving force of the TH from glycerol is largely due to the conversion of the initial dehydrogenation product of glycerol, dihydroxyacetone (DHA), to lactate via dehydration and intramolecular Cannizzaro reaction.[25, 26, 27] Consistent with this, the calculated $\Delta G°_{aq}$ for TH of bicarbonate from glycerol is also significantly more favourable than the direct hydrogenation of bicarbonate under basic conditions (-83.9 vs 4.44 kcal/mol).

[a] 800 22nd St NW, Suite 4000, Washington D.C. 20052
† Footnotes relating to the title and/or authors should appear here.
Electronic Supplementary Information (ESI) available: catalyst syntheses, crystallographic data for ***7***, and additional data on catalytic activity. See DOI: 10.1039/x0xx00000x

Scheme 1. Catalysts reported for the transfer hydrogenation of carbonates from glycerol.

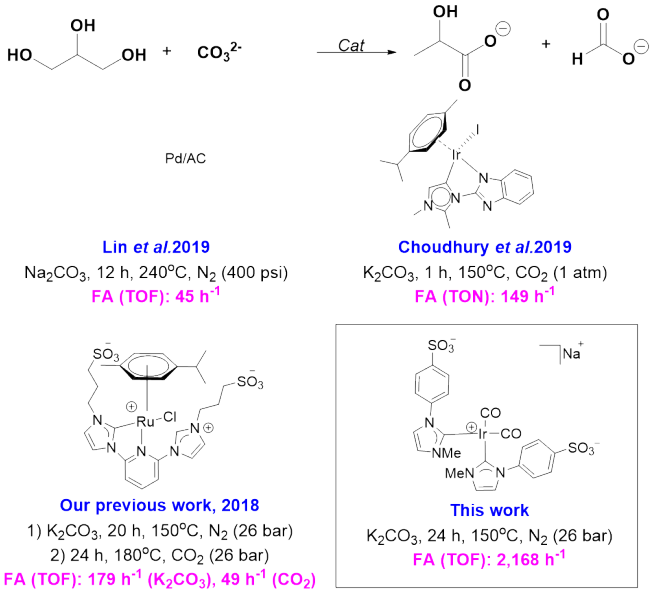

In addition to the above process advantages of using TH from glycerol, the use of glycerol as H-donor provides a route to valorization[28] of this abundant by-product of the biodiesel industry[29] to lactic acid. Demand and price for the latter continue to increase, driven by new applications in cosmetics, polymer synthesis,[30] fine chemicals and food preservation.[31] We recently reported the first homogeneous catalyst for the TH of CO_2 and carbonates from glycerol, consisting of water-soluble Ru *N*-heterocyclic carbene (NHC) complex.[22] The catalyst afforded 49 turnovers/h with 26 bar CO_2 and 180 °C, but showed higher efficiency for carbonate (179 h^{-1} with 2 M K_2CO_3 at 150 °C, Scheme 1). Since then, Choudhury et al reported an Ir-NHC (abnormal NHC) complex, achieving a TOF of 90 h^{-1} at 150 °C with K_2CO_3 and ambient CO_2 pressure.[32] Notably, the latter catalyst did not afford lactic acid as a by-product, but rather DHA. Lin *et al.* also recently reported the TH of carbonates from glycerol at 240 °C with Pd/C.[33] affording a TOF of 45 h^{-1} (Scheme 1). While the TH of carbonates has potential applications on a large scale, it requires the development of more efficient, robust catalysts and the minimization of the use of precious metals.

Towards this goal, here we report our progress on the design of highly prolific and robust homogeneous catalysts for the transfer hydrogenation of carbonate salts from glycerol, affording lactate and formate salts under basic conditions with efficiencies that compare favourably to the precedents (Scheme 1). We also report mechanistic insights on the process that will continue to inform the design of prolific catalysts precursors for transfer hydrogenation reactions of from renewable H-donors. We note that the catalysts reported here are designed to serve as precursors to site-isolated heterogeneous catalysts (SIHCs) for this reaction, which will minimize the use of the precious metal in continuous processes.

Results and discussion

Catalyst synthesis.

Eight iridium(I) and iridium(III) *N*-heterocyclic carbene (NHC) complexes, six of which bear sulfonate-functionalized wingtips (***2*** – ***7***, Scheme 2), were synthesized and characterized with the goals of (i), assessing their activity for the TH of carbonate salts from glycerol to afford lactate and formate salts; and (ii), identifying structural features of the pre-catalyst, including presence of sulfonate moieties, which are associated with higher catalytic activity and selectivity. The sulfonated iridium compounds were compared to the ruthenium sulfonated NHC complex previously reported by us (***1***)[24], as well as two non-sulfonated iridium NHC complexes (***8*** and ***9***). While exact analogues of Ir(I) and Ir(III) pre-catalysts could not be accessed synthetically in some cases (e.g. Ir(I) analogue of ***2*** proved unstable in our hands), the series depicted in Scheme 2 provides ample grounds for comparison of the effects of ligands and metal oxidation state.

Iridium(III) compounds ***2*** and ***3*** were included based on their high activity for transfer hydrogenation of aldehydes, imines, and ketones from glycerol,[25, 34] which was first reported by Peris et al. Iridium(I) compounds ***4*** – ***7***, on the other hand, were included in light of our previous reports of their high activity for acceptorless dehydrogenation of glycerol. [14, 35] Comparisons between compounds ***4*** and ***5*** elucidate the effect of the *N*-sulfonate spacer on catalytic activity and stability, while comparisons between ***4*** and ***6***, and ***5*** and ***7*** respectively speak to the effect of stronger π-acceptor CO ligands versus the weaker and more labile cyclooctadiene (*cod*) ligands. Finally, compound ***8*** and ***9*** provide insight into the effect of the sulfonate functionalization on catalyst activity.

Scheme 2. NHC catalysts examined for the transfer hydrogenation of carbonate salts from glycerol.

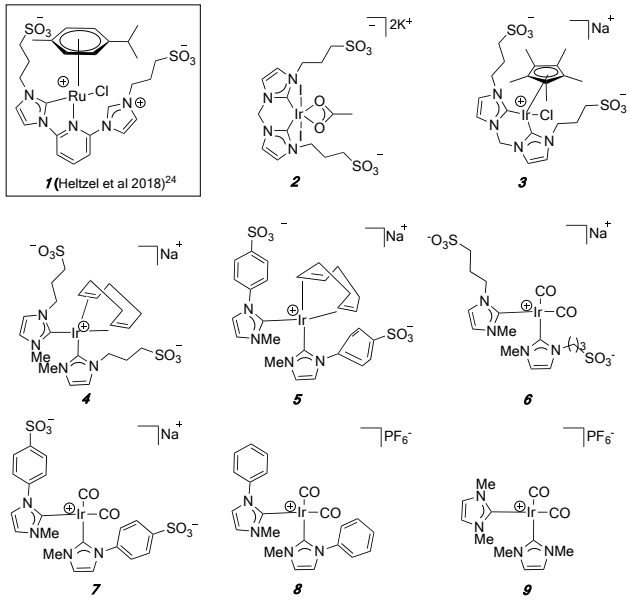

The molecular structure of ***7*** was determined by single crystal X-ray diffraction (Figure 1) and compared to our previously reported structure of the *cod* analogue ***5***. The crystal structure shows a disordered square planar coordination with two phenyl wingtips in a

staggered orientation. A closely coordinating sodium ion and several co-crystalized water molecules can also be resolved. The torsion angles between the CO-Ir plane and the carbene carbons (C(16) and C(6) respectively) are 65.865° (N4 C16 Ir1 C1) and 65.875° (N2 C6 Ir1 C2) respectively. In comparison, the symmetric analogue with *N*-methyl wingtips (***9***), reported by Crabtree et al,[35] has a larger torsion angle than ***7*** (80.78°). The Ir-C (NHC) bond distances of ***7*** measure 2.093(8) and 2.088(8) Å, marginally longer than those of the analogous *cod* complex by approximately 0.045 Å,[14] but still comparable to those reported for analogous Ir-NHC compounds, such as ***9***.[35, 36] The Ir-CO bond lengths, C(1)-Ir(1) and C(2)-Ir(1), measure 1.880(10), and 1.876(10) Å respectively, in the typical range of Ir-CO bond lengths and comparable to those in non-sulfonated compound ***9***.[35] The phenyl wingtips stagger in opposite directions with torsion angles of 41.428° (C8 C7 N1 C5) and 45.526° (C18 C17 N3 C16), compared to those of the *cod* analogue at 60.40° and 45.02°.[14] The differences in torsion angle between the two ligands can be attributed to the coordinating sodium ion and closely associated water molecules that act as a bridge between two molecular units (see ESI Figure S2 and S3 for more information).

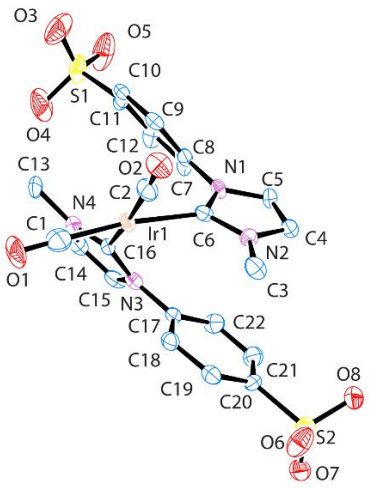

Figure 1. ORTEP diagram of one of two crystallographically unique catalyst molecules in ***7***, containing the iridium metal centre Ir1. Lattice water molecules and sodium atoms are excluded for clarity. See ESI Figure S1 and S2 for additional ORTEP illustrations. Select bond lengths (Å) and angles (deg): C(1)-Ir(1) 1.880(10), C(2)-Ir(1) 1.876(10), C(6)-Ir(1) 2.093(8), C(16)-Ir(1) 2.088(8), C(6)-Ir(1)-C(16) 86.9(3)°, C(1)-Ir(1)-C(2) 92.5(4)°.

Glycerol Transfer Hydrogenation to Carbonate Salts

We next compared the activity of the catalysts in Scheme 2 for the transfer hydrogenation for carbonate salts from glycerol. In a previous report we discussed the optimization of reaction conditions,[22] and suggested that catalytic activity for the gaseous reactions with CO_2 is often limited by mass transfer related to CO_2 or base solubility. This is further complicated by the fact that the catalyst can also facilitate acceptorless dehydrogenation, as well as pH-dependent formate dehydrogenation at low pH.[22] As a result, reaction rates for transfer hydrogenation and product selectivity have a strong dependence on temperature, pressure and base solubility. Given that CO_2, carbonate and bicarbonate are in equilibrium in the presence of aqueous base, our main focus here is on the screening of the catalysts for TH of carbonates from glycerol, with no additional base. Products were identified and quantitated with HPLC and ^{1}H NMR using an internal standard, as described in the Experimental section and ESI.

Carbonate Salts.

Initial screen for TH of potassium carbonate (K_2CO_3) from glycerol was performed with 2.7 M K_2CO_3, 1:1 water/glycerol and 0.001 mol% (10 ppm) catalyst using microwave heating to 150 °C for 6 hours. The use of microwave heating allows for more efficient screening of the catalysts and precise reaction temperature control. Carbonate was selected over bicarbonate in order to maximize initial pH (12.1). At this pH the theoretical ratios of HCO_3^-:CO_3^{2-} at pH 12.1 is 2:98, which is notable because bicarbonate is likely the only species that can undergo transfer hydrogenation.[15]

Control reactions without catalyst afford no appreciable conversion of glycerol or carbonate salts, while those without glycerol afford no carbonate conversion. In the absence of carbonate salts (or CO_2), the catalytic reactions afford only lactate salts via acceptorless dehydrogenation (AD) of glycerol, as reported previously.[14] The dehydrogenation reaction does not proceed in the absence of base. We had suggested that the base is also important for suppressing the reverse reaction, formate dehydrogenation, which we observed at pH < 4.[22] Given that many of these catalysts are active for glycerol AD, it was not surprising to observed AD as a competing process, resulting in the formation of excess lactate compared to formate. The TH and AD processes have distinct activation energies and thus temperature-dependences; as a result, the ratio of lactate:formate varies with temperature and with choice of catalyst. For example, at 150 °C with catalyst ***1*** the concentrations of lactate and formate are comparable, but above 150 °C lactate exceeds formate (ESI Figures S4a and Figure S4b).

All Ir catalysts except for 1,5-cyclooctadiene (cod) complexes ***4*** and ***5*** were more active for TH than our previously reported Ru (***1***) catalyst, which afforded 2754 and 506 turnovers for lactic and formic acid respectively in 6 hours (Figure 2). The low activity of ***4*** and ***5*** is likely associated with the labile *cod* ligand, whose dissociation may provide a route to decomposition products, such as iridium dimers previously observed by Crabtree et al.[27] Interestingly, *cod* complexes ***4*** and ***5***, which differ in *N*-substituents, also differ in TH activity: while the *N*-propyl-sulfonate analogue (***4***) is inactive for transfer hydrogenation, the *N*-phenylsulfonate analogue (***5)*** shows some (albeit low) TH activity (508 turnovers of formic acid, Figure 2).

The activity of the iridium (III) sulfonated catalysts ***2*** and ***3*** was comparable: ~ 5200 - 5300 turnovers for lactic acid and 890 - 1350 for formic acid, with ***2*** having higher activity than ***3.*** We had previously shown that adding an excess of NaOAc doubles the activity of ***3*** for AD of glycerol, suggesting that slow initial substitution of the chloride may be responsible for its inferior activity relative to ***2***.[14] The relative activity of the Ir(I) catalysts (***4*** – ***9***) was dependent on the ancillary ligand and the *N*-wingtips: as noted earlier, the *cod* complexes were significantly less active than the bis(carbonyl) analogues. This is consistent with both our prior report on glycerol AD,[14] as well as a report by Crabtree et al demonstrating that $[(IMe)_2Ir(CO)_2]BF_4$ (IMe is 1,3-dimethylimidazole-2-ylidene) had higher activity than corresponding *cod* complex for this process.[35] While both sulfonated carbonyl derivatives ***6*** and ***7*** were more active than their *cod* precursors (***4*** and ***5***, Figure 2), the relative

improvements were not equal. Compound ***7***, with *N*-phenylsulfonate wingtips, showed ~ 7-fold higher activity for production of lactic acid than *cod* analogue ***5***, and ~16-fold for formic acid, far exceeding the improvement in activity of ***6*** over ***4***. We attribute this to the higher thermal stability of the *N*-phenylsulfonate in ***7*** to degradation via Hoffman elimination compared to the N-propylsulfonte in ***6***.[37, 38] More thermally robust catalysts should have a significant advantage in catalyst lifetime under microwave conditions, where superheating can result in formation of hotspots.

Consequently, the overall highest activity for transfer hydrogenation was observed with ***7*** (15400 and 8120 turnovers for lactic and formic acid respectively, compared to 2780 and 810 turnovers respectively for ***6***. The TOF of formic acid afforded by ***7*** (1353 h^{-1}) is ~ 16-fold higher than the activity of our previously reported Ru catalyst (***1***) under these conditions (84 h^{-1}) and the Ir-NHC catalyst by Choudhury et al (90 h^{-1}).[32]

Scheme 3.

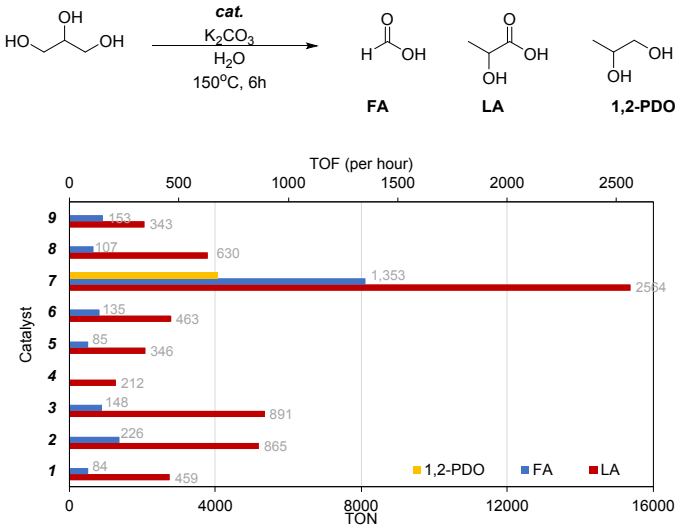

Figure 2. Activity of NHC catalysts ***1*** – ***9*** (Scheme 2) for transfer hydrogenation of K_2CO_3 from glycerol, based on observed turnover numbers (TON) and turnover frequencies (TOF) of for FA, LA and 1,2-PDO (labels in grey refer to TOF per hour). Conditions: 1: 1 water: glycerol (6.84 M), K_2CO_3 (2.7M), <0.001 mol% catalyst, 150 °C, 6 h. Quantified by HPLC and NMR.

Catalyst ***7*** was also the only one that produced significant amounts of 1,2-propanediol (1,2-PDO) as a side product, with 4080 turnovers, resulting in a selectivity ratio of ~1:2:4 for 1,2-PDO:formic:lactic acid. The formation of 1,2-PDO is attributed to transfer hydrogenation of a dehydration products of glycerol, α-hydroxyacetone (Scheme 4), or the double hydrogenation of pyruvaldehyde. Neither of these could be identified as an intermediate by HPLC or NMR, likely because under reaction conditions both would undergo transfer hydrogenation from isopropanol. In fact, pyruvaldehyde afford a 95:5 product mixture of lactate to 1,2-PDO using catalyst ***7***, isopropanol and base. While this result does not provide direct evidence for the fact that 1,2-PDO is formed via pyruvaldehyde, it is consistent with the latter hypothesis. We also considered the possibility that the 1,2-PDO is produced from lactic acid through transfer hydrogenolysis. However, a comparable experiment with lactic acid and isopropanol as hydrogen donor afforded no 1,2-PDO, suggesting this pathway is less likely than those via pyruvaldehyde or α-hydroxyacetone (Scheme 4).

The fact that no 1,3-PDO was observed suggests that glycerol dehydration is selective. This observed selectivity is likely associated with the more thermodynamically favourable dehydrogenation/hydrogenation to the 1,2-PDO vs the 1,3-PDO, as suggested by calculations of the Gibbs free energies of reaction ($\Delta\Delta G°_{aq}$ 5.4 kcal/mol, ESI Table S3).

We sought further insight into selectivity trends by comparing the catalysts in terms of the excess of acceptorless hydrogenation (AD) activity relative to transfer hydrogenation (TH) activity. As such, we can define two relative excess terms, as follows:

$$excess_{AD/TH} = \frac{[LA] - ([FA] + [1,2\text{-PDO}])}{[FA] + [1,2\text{-PDO}]} \times 100 \quad (1)$$

and

$$excess_{AD/FA} = \frac{[LA] - [FA]}{[FA]} \times 100 \quad (2)$$

where [LA], [FA] and [1,2-PDO] refer to the concentrations of lactic acid, formic acid and 1,2-PDO at a given time in the reaction. Equation 1 quantitates the relative excess of AD over TH resulting in both observed TH products (FA and 1,2-PDO), whereas equation 2 refers specifically to transfer hydrogenation to yield formic acid. The two values are identical for all catalysts except ***7***, given that only ***7*** affords 1,2-PDO as a second TH product. The values for $excess_{AD/TH}$ are lowest for ***7*** (26%), and highest for the Ir(III) complex ***3*** (503%), while $excess_{AD/FA}$ for ***7*** is 89% (ESI Table S4). The latter analysis suggests that catalyst ***7*** is not only the most efficient for AD of glycerol, but also for transferring the H-equivalents to an acceptor. However, the trends for TH and AD are not parallel for the catalyst series, as summarised below:

TH activity (formic acid): ***7*** > ***2*** > ***3*** > ***9*** > ***6*** > ***8*** > ***5*** > ***1*** > ***4***
AD activity: ***7*** > ***3*** > ***2*** > ***8*** > ***6*** > ***1*** > ***5*** > ***9*** > ***4***

Scheme 4. Proposed route to lactic acid, formic acid and 1,2-PDO from glycerol transfer hydrogenation of carbonates.

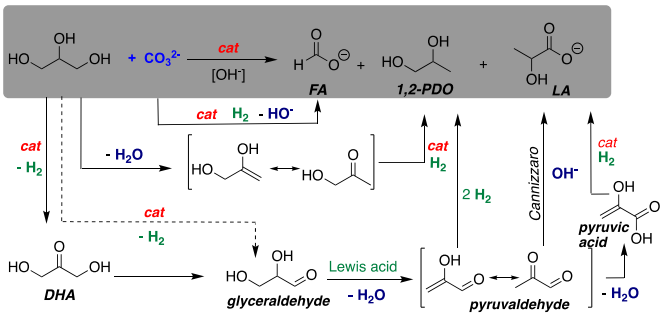

Sulfonate effect

We further examined the effect of the sulfonate group by comparing the dehydrogenation activity of ***7*** to that of the non-sulfonated analogue, ***8***, as well as ***6*** to ***9*** (Scheme 2). Compound ***8*** affords 3780 and 644 turnovers of lactic and formic acid respectively, which is approximately a 4-fold decrease in lactic and 12-fold decrease in formic acid compared to ***7***. Catalyst ***8*** also has a much

higher *excess*$_{AD/FA}$ (487%, see eq 1 and Table S4). Interestingly, the activity of ***6*** vs ***9*** was much more comparable (2780 vs 2060 turnovers of lactic acid, and 810 vs 918 of formic acid for ***6*** and ***9*** respectively). Sulfonated and non-sulfonated Iridium(III) NHC catalysts have shown similar trends for the acceptorless dehydrogenation of glycerol. We had previously shown that the non-sulfonated analogue of ***3***, possessing n-propyl wingtips, was ~50% less active in acceptorless dehydrogenation of glycerol relative to ***3***.[26] We suggest that the effect of the sulfonate group is driven by solubility differences in aqueous media: thus, in the case of ***7*** vs ***8***, the increase in aqueous solubility that results from addition of the sulfonate groups is expected to be more significant than that of in ***6*** vs ***9*** due to the more lipophilic nature of the phenyl vs propyl groups, as indicated by the octanol-water partition coefficients for the propyl vs phenyl analogues (-5.57 and -3.81 respectively, calculated by ChemAxon Marvin Suite). The lower aqueous solubility is likely to favour formation of inactive CO-bridging dimers, as observed by Crabtree et al for an NHC catalyst.[27]

Carbonate concentration.

We briefly explored the effect of carbonate concentration to the catalytic activity of ***7***. While maintaining a glycerol concentration of 6.84 M in a 1:1 glycerol:water mixture, K_2CO_3 concentration was varied from 0 to 2.7 M, at which point saturation was reached. As carbonate concentration is increased, rates of formation of lactic and formic acid increase correspondingly (Figure 3). In addition, we observe a decrease in the relative excess of TH vs AD (excess$_{AD/TH}$), from 117% at 0.5 M K_2CO_3 to 26% at 2.7 M. The increase in overall reaction rate is consistent with the involvement of hydroxide in the last step of the Cannizzaro reaction leading to lactic acid formation (Scheme 4). The lactic acid formation also provides additional thermodynamic driving force for the overall process.[24] The increase in TH rate is also consistent with the expected effect of increasing substrate (i.e. carbonate) concentration. The rate of formation of the secondary TH product, 1,2-PDO, also increases at higher carbonate concentration but by significantly less than the that of formate production. The latter is not surprising, since higher carbonate concentration results in higher abundance of carbonate as a competing hydrogen acceptor. The small increase in 1,2-PDO could also reflect the need for base to facilitate glycerol dehydrogenation, the first step in 1,2-PDO formation (Scheme 4).

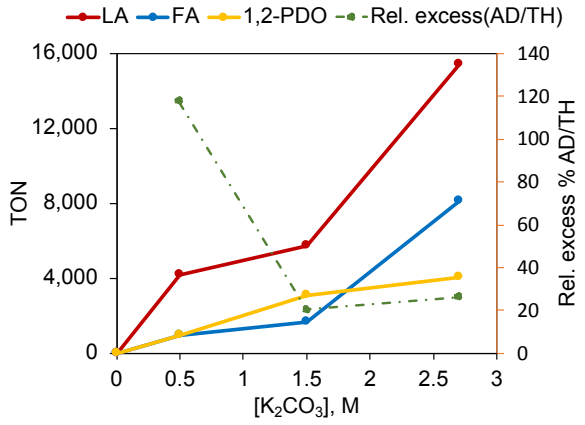

Figure 3. TON of FA, LA and 1,2-PDO observed in reactions at different concentration of K_2CO_3 using catalyst ***7***. Conditions: 1: 1 water: glycerol (6.84M), K_2CO_3 (specified concentration), <0.001 mol% ***7***, 150 °C, 6 h.

Carbonate salt effect

The initial results with potassium carbonate led us to consider the potential effect of changing the carbonate cation. To that end, carbonate salts of the alkali earth metal series (Li, Na, K and Cs) were tested using catalyst ***7*** under the microwave conditions described above (150 °C, 6 hours). However, we observed significant differences in solubility of these salts in the reaction medium. These differences were justified by measuring the saturation concentrations of the carbonates in the reaction medium (Li_2CO_3: 0.33 M, Na_2CO_3: 1.3 M, K_2CO_3: 3.6 M and Cs_2CO_3: 5.3 M). Thus, not surprisingly, the TONs obtained associated with the dehydrogenation product (lactic acid) and the sum of hydrogenation products (formic acid and 1,2-PDO) were found to increase as we change the salt cation from Li to Cs (Figure 4 and Table S6): for example, relative to the TONs afforded by Li_2CO_3 (2530 and 146 for lactic and total transfer hydrogenation products respectively), Cs_2CO_3 affords 27 850 and 27 840 turnovers respectively. Glycerol conversion correspondingly increases – for example, 2% for Li_2CO_3 vs 26% for Cs_2CO_3 (ESI Table S6). Given that only the Cs_2CO_3 and K_2CO_3 reactions were fully homogeneous, we can only compare their kinetics. Given that the concentration of salt used was below saturation for both K_2CO_3 and Cs_2CO_3, differences in reaction rates between these two are not accounted for by solubility of the carbonate salt. Interestingly, the relative acceleration of TH is higher than that of dehydrogenation (e.g. moving down the group from K to Cs increases lactic acid TONs by 180%, and those associated with the dehydrogenation products (formic acid and 1,2-PDO) by 228%. As a result, the relative excess of AD to TH (excess$_{AD/TH}$) drops from 1636% for Li to ~0% for Cs, as we change cations down the alkali metal series (Figure 3). The latter implicates the cation in participating in a rate-determining step in the catalytic cycle associated with hydrogenation, consistent with prior reports of cation effects on CO_2 and carbonate hydrogenation.[16, 19, 24]

In addition, we observe that the rates of formation of the two transfer hydrogenation products (formic acid and 1,2-PDO) are not accelerated equally: the increase in 1,2-PDO TONs is approximately double that of FA TONs from K to Cs (Li_2CO_3 affords no 1,2-PDO). This results in a decrease in the selectivity for formic acid vs 1,2-PDO from to 48% for Cs. The greater acceleration associated with 1,2-PDO relative to FA implicates the cation in both the dehydration of glycerol to α-hydroxyacetone and the TH of the latter to 1,2-PDO (Scheme 4).

We also considered the fact that the reaction rate would be affected by the difference in aqueous solubility of the salts (ESI Table S5) with increase in the effective ionic radius of the cation. As previously noted, Li_2CO_3 and Na_2CO_3 are not fully dissolved at the beginning of the reaction. Furthermore, the stability of the product lactate and formate salts are likely to be more favourable with more polarizable cations, such as Cs^+. While the latter arguments could account for the increase in formic and lactic acid, they do not readily account for the increase in rate of 1,2-PDO formation. As observed previously, increasing K_2CO_3 concentration had only a limited effect on the rate of 1,2-PDO formation (Figure 3). In contrast, changing the cation down the group results in an increase of 1,2-PDO double that of the corresponding increase in TONs of FA (Figure 4).

To probe whether Cs^+ can be used in catalytic quantities to obtain similar effects, we performed an experiment with a 9:1 ratio of K_2CO_3:Cs_2CO_3, which affords activity comparable to that obtained with Cs_2CO_3 alone (22 200 and 12 660 turnovers of lactic and formic respectively, compared to 27 850 and 13 350 – entries 6 and 3, ESI Table S6). The addition of 10% Cs_2CO_3 increases lactic and formic acid production ~ 1.5-fold compared to an experiment with equivalent concentration of K_2CO_3 (Figure 4, right panel), and only 4% relative excess of AD over TH. Glycerol conversion follows suit -– for example, 26% for Cs_2CO_3 vs 21% for 9:1 K_2CO_3:Cs_2CO_3.These results further suggest that Cs^+ can be used in catalytic quantities to accelerate lactic acid and formic acid formation, but effect on 1,2-PDO formation is more concentration-dependent. We also examined whether the presence of harder Lewis acids, such as Li^+, suppresses activity via inhibitory effects. A reaction with 9:1 ratio of Li_2CO_3:Cs_2CO_3 resulted in only a ~ 10% reduction in lactate and formate compared to the control with K_2CO_3 alone (Figure 4, right panel), suggesting that the main driver of the low TONs obtained with Li_2CO_3 is low solubility. Consistent with this conjecture, we recover ~ 90% of the original mass of Li_2CO_3 at the end of the reaction as undissolved carbonate.

Thus, we conclude that the stark effect observed in reaction rate by changing the alkali earth metal ion of the carbonate salts is a combination of increasing solubility with increasing polarizability of the cation, as well as specific roles in the facilitating a rate-determining step in the catalytic cycle associated with TH and the dehydration of glycerol to α-hydroxyacetone, the H-acceptor precursor to 1,2-PDO.

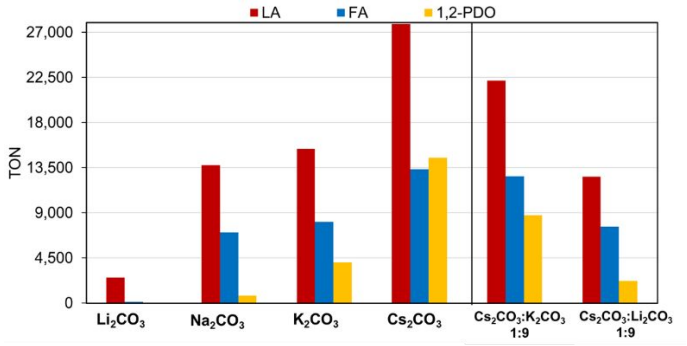

Figure 4. Effect of carbonate source on the TONs of formic acid (FA), lactic acid (LA) and 1,2-propanediol (1,2-PDO) using catalyst ***7***. Raw data presented in ESI Table S4. [Conditions: 1: 1 water: glycerol (6.84 M), [M_2CO_3]: 0.03 M for Li_2CO_3, 1.3 M for Na_2CO_3 and 2.7 M for K_2CO_3 and Cs_2CO_3, <0.001 mol% ***7***, 150 °C, 6 h, microwave.]

Solvent effect.

We also investigated the effect of water on catalyst activity and selectivity. The choice of solvent for initial screening was 1:1 water:glycerol, selected so as increase solubility of carbonate salts and reduce viscosity of neat glycerol. Although these effects should benefit reaction rate, the mechanism in Scheme 4 involves a number of dehydration steps, which could make the effect of water on the system more complex. Reactions performed in neat glycerol all showed small decrease in amounts of lactate produced relative to the 1:1 water:glycerol reactions with the same salt (12% and 30% for Na_2CO_3 and K_2CO_3 respectively) and a small increase in formate produced (Figure 5, 33% for Na_2CO_3). Notably, however, neither neat reaction produced any 1,2-PDO. In the case of the neat reaction with Cs_2CO_3 we observed more significant decreases in both the lactate and formate production (~50% reduction in both), and no 1,2-PDO production. The suppression of 1,2-PDO formation under neat condition suggests a strategy that can be used to increase selectivity for formic acid, especially in the reaction with Cs_2CO_3.

Mechanistically, the effect of neat conditions on suppressing 1,2-PDO production could be due to the fact that in the absence of water, carbonate cannot hydrolyse to form bicarbonate and hydroxide:

$$CO_3^{2-} + H_2O \rightarrow HCO_3^- + HO^-$$

The Bronsted acidic bicarbonate may be necessary to facilitate the dehydration of glycerol to α-hydroxyacetone, the precursor to 1,2-PDO. Although there is also a dehydration step in the generation of lactic acid (glycerealdehyde to pyruvaldehyde, Scheme 4), that step is more thermodynamically favourable due to formation of a conjugated product, and thus be may be facilitated by weak Lewis acids. If hydrolysis to bicarbonate is indeed suppressed in neat glycerol, we must reconsider whether bicarbonate is indeed the true substrate for TH to formate, or whether carbonate can bind to the catalyst and be protonated from glycerol.

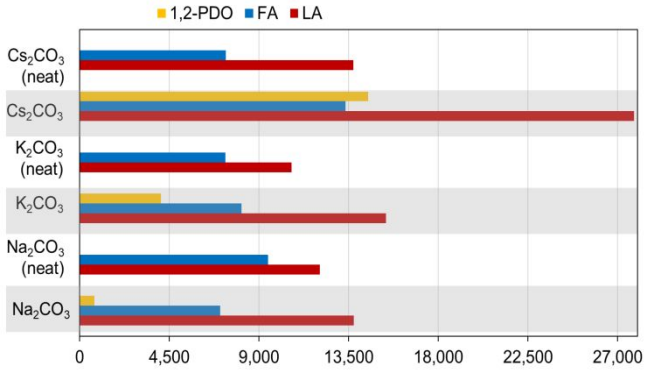

Figure 5. Comparison of TONs of formic acid (FA), lactic acid (LA) and 1,2-propanediol (1,2-PDO) obtained using aqueous glycerol (1:1) and neat glycerol conditions using catalyst ***7***. [Conditions: Neat glycerol or 1:1 water:glycerol, as indicated; <0.001 mol% ***7***, carbonate salt (2.7 M) 150 °C, 6 h, microwave.]

TH of carbonates using conventional heating.

We further explored the activity of catalyst ***7*** under conventional heating conditions at the same temperature as the microwave reactions. In order to keep all components in the liquid phase the reactions were performed in a Parr reactor under N_2 pressure, keeping all other conditions consistent with the microwave reactions and extended the reaction time (1:1 glycerol/water, 2.7 M K_2CO_3 at 150 °C). Under conventional heating and 26 bar N_2 the TONs of LA and FA observed after 6 hours are approximately double compared to those obtained in the microwave reaction (27 760 vs 15 380 for LA and 16 630 vs 8120 for FA, 8% conversion of glycerol (Figure 6 and ESI Table S5). The glycerol conversion closely matches the sum of lactic acid and 1,2-PDO yields, suggesting high selectivity for these two products. This is accompanied by a higher selectivity for FA over 1,2-PDO under the conventional conditions (~3:1 vs 2:1). In 24 hours, the reaction reaches 72 250 turnovers of LA and 52 030 of FA (TOF of 2170 h^{-1}). The 1,2-PDO concentration reaches a steady state after the first 6 hours of reaction, while LA and FA concentrations steadily rise (Figure 6). As a result, the selectivity for FA vs 1,2-PDO increases over the course of the reaction, reaching 23:1 after 24 hours (Figure 6a). The relative excess of AD over the sum of the two TH products, which

should be minimized in order to optimize catalyst selectivity, steadily decreases over the course of the reaction from 286% to 33%, tracking the decrease in pH from 12.2 to 11.4 (ESI Figure S5).

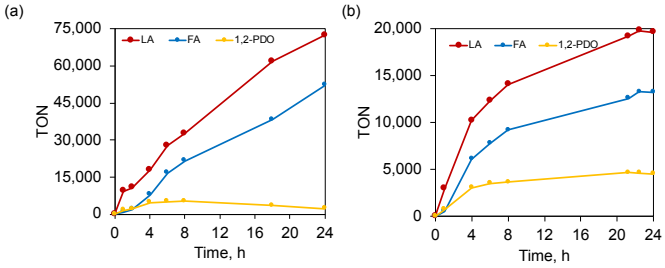

Figure 6. Time course for production of formate, lactate and 1,2-PDO from the reaction of glycerol using catalyst ***7,*** 6.85 M aqueous glycerol, 2.70 M K_2CO_3, 0.001 mol% ***7***, 150 °C, N_2 pressure (a) 26 bar and (b) 50 bar.

We hypothesized that the reason for the increase in activity under the latter conventional conditions vs microwave conditions was related to the applied N_2 pressure. The effect of the positive pressure is complex, especially at elevated temperatures. Initially we postulated that the higher pressure may result in decreased solubility of the carbonate salt; however, this effect is likely to be small for a pressure difference of 26 to 50 bar relative to the internal pressure of liquids.[39] Potential evidence for this was found in pH measurements over the course of both reactions, which show that the 50-bar reaction has pH values 0.6 – 0.8 units lower than that of the 26-bar reaction (ESI Figure S5). While the pH drop could also be due to formation of acid products, the higher reaction rate in the 26-bar reaction contradicts that. In sum, we conclude that the TH to afford FA proceeds more efficiently and selectively in a pressure reactor, where the effect of external pressure can be optimized to increase availability of carbonate without compromising solubility of the base.

Mechanism of Ir-catalysed TH

The identification of the Ir(I) compound ***7*** as the most active catalyst for both TH and AD led us to consider possible mechanisms for both reactions and how they may differ from established mechanisms for the more extensively studied Ir(III) catalysts. For Ir(III) and Ir(I) catalysts with open coordination sites, TH typically proceeds via ligand substitution by an alkoxide, followed by ß-hydride elimination to form a hydride and insertion of the H-acceptor into the hydride. Release of H_2 has been proposed to proceed via hydride abstraction using H^+.[40] Such a mechanism cannot be applied to ***7***, as the 16-electron square planar d^8 complex lacks open coordination sites. Furthermore, dissociation of CO is likely to be prohibitive due to the high calculated and experimentally-determined BDEs for similar Iridium species.[41, 42] Dissociation of the NHCs is also expected to be prohibitive, with typical BDEs > 60 kcal/mol.[43] However, in search of experimental evidence that for potential ligand dissociation, we performed a reaction with excess imidazolium salt, which under the strongly basic conditions would be expected to facilitate NHC formation. This would lead to decreased reaction rate if M-NHC dissociation were involved in catalyst activation. However, no significant difference was observed in the rate from the control experiment, suggesting that the catalytic cycle does not involve NHC dissociation.

Thus, we propose the mechanism shown in Figure 7. In order to associate the H-donor (glycerol), the 16-electron Ir(I) species can undergo O-H oxidative addition of the primary or secondary hydroxyl to form an alkoxy hydride complex, which has precedents for Ir(I) complexes.[44] If the mechanism involves ß-hydride elimination, the resulting saturated Ir(III) alkoxy hydride complex (previously observed by NMR)[14] must open up a site.[45] The latter could more readily dissociate a carbonyl compared to the Ir(I) species, given that expectedly lower M-CO bond dissociation energy due to decreased backbonding from the more oxidized iridium. To seek evidence for CO dissociation we performed LC-MS at various times during the reaction to identify prevalent iridium fragments. We were able to identify a fragment consistent with mass of $[(NHC)_2Ir(CO)(DHA)H_2]^-$ (DHA = dihydroxyacetone), suggesting CO loss upon glycerol coordination and ß-hydride elimination. Thus, the CO dissociation would allow the alkoxy glycerol complex to have an open site necessary for ß-hydride elimination, forming DHA or glyceraldehyde. The identity of the intermediate has not been determined here as we have not been able to spectroscopically observe either in sufficient concentration. This is likely because both DHA and glyceraldehyde rapidly react under reaction conditions to form lactic acid. However, we postulate the intermediate is more likely to be DHA, as the glycerol dehydrogenation at the secondary alcohol is thermodynamically more favourable than that of primary by (-5.11 kcal/mol vs 0.17 kcal/mol respectively). Furthermore, even if glyceraldehyde is the kinetic product, rapid isomerization to DHA will be driven by the favourable thermodynamics.

Either product can be displaced by bicarbonate via ligand substitution. Unfortunately, we have not been able to observe either (DHA nor glyceraldehyde) under basic conditions, likely because both quickly react to form lactate via dehydration and intramolecular Cannizzaro reaction.[35]

Coordinated bicarbonate undergoes hydroxide elimination; such a step has been previously proposed by DFT calculations for the Ru-catalysed hydrogenation of bicarbonate.[46] The resulting H-Ir-CO_2 complex undergoes insertion[46, 47] to generate iridium formate, possibly trapped by re-coordination of CO (Figure 7). It is also possible though that CO re-coordination may not be feasible at the very low catalyst concentrations (and thus CO concentrations) used here. Thus, an alternative to the cycle is possible, where CO does not re-coordinate. In the latter scenario after initial CO loss, subsequent cycles would not involve CO dissociation. Finally, reductive elimination releases the formic acid, which is rapidly deprotonated under basic conditions, and reforms the Ir(I) species.

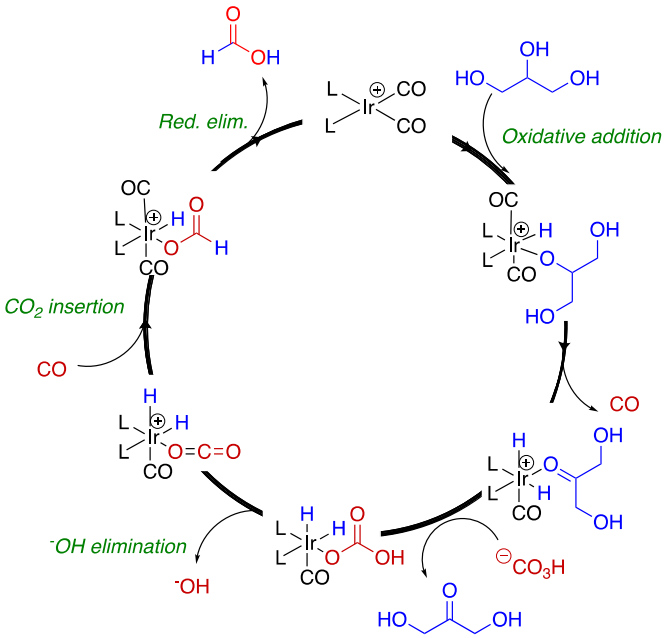

Figure 7. Proposed catalytic cycle for transfer hydrogenation of bicarbonate with glycerol by catalyst ***7***. Note that it has not been determined definitely whether the intermediate dehydrogenation product of glycerol is DHA or glyceraldehyde.

The latter analysis suggests that catalyst ***7*** is not only the most efficient for AD of glycerol, but also for transferring the H-equivalents to an acceptor.

The lower activity of $[(NHC\text{-}Ph\text{-}SO_3)_2Ir(cod)]^-$ (***5***) vs $[(NHC\text{-}Ph\text{-}SO_3)_2Ir(CO)_2]^-$ (***7***) for both acceptorless dehydrogenation, but especially for transfer hydrogenation (see Figure 2) could be attributed to several factors: (i) more favourable reductive elimination of formic acid from Ir center in ***7*** with stronger π-acceptor (CO) ligands; (ii) more favourable insertion of CO_2 into Ir-H with more electron-withdrawing CO ligands, or (iii) the fact that ***5*** undergoes an entirely different mechanism than ***7*** via displacement of the cycooctadiene ligand. Although the presence of carbonyl ligands in ***7*** also opens the possibility for cluster formation[37, 41] this is not as likely at the low catalyst loadings (10 ppm) used compared to prior reports. [35, 48] It is also possible that cluster formation is more favoured for catalysts that have low solubility in the reaction medium.

Experimental

General considerations and instrumentation

The syntheses of the catalysts were carried out under nitrogen using standard Schlenk technique. Commercial chemicals were used without further purification. $[RuCl_2(p\text{-cymene})]_2$ and $IrCl_3$ were purchased from Acros-Organics. Solvents were dried using a solvent purification system (SPS MBraun) or 4 Å molecular sieves. Glycerol (>99%, Alfa Aesar) was dried over activated 4 Å molecular sieves. KOH (purity 85%) was obtained from VWR BDH, while NaOH (purity 97%) was obtained from VWR Life Science. Potassium formate (99%) was obtained from Alfa Aesar. Isopropanol (HPLC grade) was obtained from Fischer Scientific.

NMR spectra were recorded on an Agilent NMR spectrometer operating at 400 MHz. GC-FID analyses were performed on an Agilent 6890N GC System with Agilent 7693 autosampler. GC-MS analyses were performed on a Shimadzu QP2010S GC-MS, while LC-MS analyses were performed on a Shimadzu LC-MS-105 single quad with a 2020 detector. Compound identity and purity were established based on ^1H and ^{13}C NMR data, HPLC, GC-FID and GC-MS. Air-free manipulations were performed using Schlenk technique or in an MBraun Pure Lab HE Inert glove box system.

Catalyst synthesis

Compounds ***1***, ***2***, ***3*** and ***5*** were prepared by silver transmetallation from the corresponding imidazolium salts, while ***4*** was synthesized by direct metalation using $[Ir(cod)OMe]_2$.[25] Compounds ***1-7*** and ***9*** were synthesized as previously described protocols by us and others,[49] while ***8***, a new compound, was prepared from the $[Ir(cod)OEt]_2$ dimer using a method analogous to that reported by Hermann and Jimenez[14, 50] For bis-NHC Ir(I) complexes ***4*** – ***8***, we found that the addition of the imidazolium salt to the iridium dimer affords cleaner formation of the target compounds than the more common Ag transmetalation method. All catalyst syntheses are described in the ESI.

General procedure for transfer hydrogenation of carbonate salts from glycerol

Microwave reactions: In a typical procedure, a 10-mL microwave vial was charged with a stir bar, 2 mL glycerol, 2 mL H_2O, K_2CO_3 (2.7 M) and catalyst (200 µL of 0.63 mM aqueous solution). The reaction mixture was heated to 150 °C for 6 hours in an Anton Paar Monowave microwave with a stir rate of 600 rpm. The products were quantified using HPLC and NMR.

Batch reactions: All reactions were carried out in a high temperature-pressure autoclave (Parr®, 4564 series) fitted with a glass insert, standard mechanical agitator, and liquid sampling tube. The glass insert was loaded with catalyst, 25 mL of aqueous K_2CO_3 (of desired concentration) and 25 mL of glycerol. The glass insert was then placed into the autoclave. The autoclave was sealed, and the stirrer turned on and set to 50% power. The autoclave was purged 3 times with N_2 (Roberts Oxygen, industrial grade) and pressurized to 10 bar. When the reaction reached the desired temperature, the pressure was adjusted to the desired operating conditions, typically 26 Bar.

Product Characterization

Reaction aliquots were analysed by HPLC and NMR. HPLC was performed using a Shimadzu Prominence-I (LC-2030C 3D) instrument equipped with a PDA and RI detectors using a mobile phase of 0.005 M H_2SO_4 with a flow rate of 0.44 mL/min at 35 °C. Samples for quantification of lactic acid (LA), formic acid (FA), 1,2- propanediol (1,2-PDO) and glycerol were prepared by adding a 1-mL aliquot of sample to 0.22 mL of 5 M H_2SO_4 and filtering with a syringe filter. The PDA detector scanned the range of 190 - 800 nm, affording traces at 190, 218, 254, and 284 nm for analysis. The 190-nm wavelength trace included glycerol and all the desired products, while the 218-nm trace excluded glycerol and 1,2-PDO. Glycerol was quantitated using the Refractive Index (RI) detector. Typical HPLC trace and PDA chromatograms are shown in Figure S6. The retention times for LA, glycerol, FA and 1,2 PDO are 28.7, 29.5, 30.5, and 36 min respectively.

NMR was used to confirm HPLC yields and identity of products. For NMR analysis, a 0.100-mL aliquot of reaction solution was mixed with equal volume of standard solution of 3-(trimethylsilyl)propionic-2,2,3,3-d_4 acid sodium salt (TSP) and 0.5 mL D_2O. The only products identified by NMR were glycerol, LA, FA, 1,2-PDO and pyruvaldehyde (in minute amounts). A comparison was made with reactions in which the TSP standard was added at the beginning of reaction, rather than to each aliquot, and no major differences were observed.

Conclusion

Here we report the design of highly prolific and robust homogeneous catalysts for the transfer hydrogenation of carbonate salts from glycerol, affording lactate and formate salts under basic conditions with efficiencies that exceed those of the few literature precedents. The most active catalyst identified is a water-soluble Ir(I) *N*-heterocyclic carbene complex (catalyst ***7***) whose activity was examined at low catalyst loading (10 ppm) at 150 °C under microwave and conventional heating in 1:1 water:glycerol. The microwave reaction with ***7*** affords lactic acid, formic and some smaller quantity of a dehydration-transfer hydrogenation product, 1-2-propanediol (1,2-PDO). The cation of the carbonate salt impacts catalytic activity and selectivity significantly, with highest activity observed with Cs_2CO_3 (27850 and 13350 TONs for lactate and formate respectively in 6 hours, compared to 15400 and 8120 with K_2CO_3, but lower selectivity for formic acid over 1,2-PDO. However, catalytic amounts of Cs^+ significantly enhance activity with K_2CO_3 to levels comparable to those obtained with Cs_2CO_3. The reaction affords high selectivity for FA more efficiently in a pressure reactor with conventional heating, where the external pressure can be manipulated to optimize carbonate concentration and solubility. High TONs for LA and FA (72,245 for LA and 52,032 for FA) were obtained with 26 bar N2 at 150 °C in 24 hours**.** Under neat conditions we observed an increase in the selectivity for FA over 1,2-PDO, especially in the reaction with Cs_2CO_3. A mechanism is proposed for TH of carbonate from glycerol using ***7,*** which involves O-H oxidative addition of glycerol, β-hydride elimination, bicarbonate dehydroxylation, CO_2 insertion and reductive elimination of formic acid. In sum, we report a highly efficient catalytic reaction that uses carbonate salts, in place of carbon dioxide, to generate formic acid via transfer hydrogenation processes from renewable H-donors such as glycerol.

Conflicts of interest

No conflicts of interest are reported.

Acknowledgements

The authors sincerely thank NSF for funding through NSF CAREER award 1554963. We thank the Prof. Cahill (GWU Chemistry) and his group for access to X-ray crystallography and assistance in data analysis.

Notes and references

[1] M. G. Mura, L. D. Luca, G. Giacomelli, A. Porcheddu, *Adv. Synth. Catal.* **2012**, *354*, 3180-3186.
[2] J. Albert, A. Jess, C. Kern, F. Pöhlmann, K. Glowienka, P. Wasserscheid, *ACS Sustain. Chem. Eng.* **2016**, *4*, 5078-5086.
[3] K. Sordakis, C. Tang, L. K. Vogt, H. Junge, P. J. Dyson, M. Beller, G. Laurenczy, *Chem. Rev.* **2018**, *118*, 372-433.
[4] P. Haynes, L. H. Slaugh, J. F. Kohnle, *Tett. Lett.* **1970**, *11*, 365-368.
[5] P. G. Jessop, T. Ikariya, R. Noyori, *Chem. Rev.* **1995**, *95*, 259-272; C. M. Jens, M. Scott, B. Liebergesell, C. G. Westhues, P. Schäfer, G. Franciò, K. Leonhard, W. Leitner, A. Bardow, *Adv. Synth. Catal.* **2019**, *361*, 307-316.
[6] I. Jószai, F. Joó, *J. Mol. Cat. A* **2004**, *224*, 87-91.
[7] P. Munshi, A. D. Main, J. C. Linehan, C.-C. C. Tai, P. G. Jessop, *J. Am. Chem. Soc.* **2002**, *124*, 7963-7971; C. A. Huff, M. S. Sanford, *ACS Catal.* **2013**, *3*, 2412-2416; G. A. Filonenko, M. P. Conley, C. Copéret, M. Lutz, E. J. M. Hensen, E. A. Pidko, *ACS Catal.* **2013**, *3*, 2522-2526; G. H. Gunasekar, K.-D. Jung, S. Yoon, *Inorg. Chem.* **2019**, *58*, 3717-3723; W. C. SHEN Zheng, LIU Shiyang, ZHANG Wei, HUANG Xin, ZHANG Yalei, *ACTA PETROL. SIN.* **2018**, *34*, 897-903.
[8] K. Rohmann, J. Kothe, M. W. Haenel, U. Englert, M. Hölscher, W. Leitner, *Angew. Chem. Int. Edit.* **2016**, *55*, 8966-8969.
[9] J. F. Hull, Y. Himeda, W. H. Wang, B. Hashiguchi, R. Periana, D. J. Szalda, J. T. Muckerman, E. Fujita, *Nat. Chem.* **2012**, *4*, 383-388; N. Onishi, S. Xu, Y. Manaka, Y. Suna, W.-H. Wang, J. T. Muckerman, E. Fujita, Y. Himeda, *Inorg. Chem.* **2015**, *54*, 5114-5123; R. Tanaka, M. Yamashita, K. Nozaki, *J. Am. Chem. Soc.* **2009**, *131*, 14168-+; S. Takaoka, A. Eizawa, S. Kusumoto, K. Nakajima, Y. Nishibayashi, K. Nozaki, *Organometallics* **2018**, *37*, 3001-3009.
[10] A. Boddien, D. Mellmann, F. Gärtner, R. Jackstell, H. Junge, P. J. Dyson, G. Laurenczy, R. Ludwig, M. Beller, *Science* **2011**, *333*, 1733-1736; Y. Zhang, A. D. MacIntosh, J. L. Wong, E. A. Bielinski, P. G. Williard, B. Q. Mercado, N. Hazari, W. H. Bernskoetter, *Chem. Sci.* **2015**, *6*, 4291-4299; C. Federsel, A. Boddien, R. Jackstell, R. Jennerjahn, P. J. Dyson, R. Scopelliti, G. Laurenczy, M. Beller, *Angew. Chem. Int. Ed.* **2010**, *49*, 9777-9780.
[11] S. Muthuramalingam, M. Sankaralingam, M. Velusamy, R. Mayilmurugan, *Inorg. Chem.* **2019**, *58*, 12975-12985.
[12] Y. M. Badiei, W. H. Wang, J. F. Hull, D. J. Szalda, J. T. Muckerman, Y. Himeda, E. Fujita, *Inorg. Chem.* **2013**, *52*, 12576-12586; S. A. Burgess, K. Grubel, A. M. Appel, E. S. Wiedner, J. C. Linehan, *Inorg. Chem.* **2017**, *56*, 8580-8589.
[13] S. Ogo, R. Kabe, H. Hayashi, R. Harada, S. Fukuzumi, *Dalton T.* **2006**, 4657-4663.
[14] M. Finn, J. A. Ridenour, J. Heltzel, C. Cahill, A. Voutchkova-Kostal, *Organometallics* **2018**, *37*, 1400-1409.
[15] F. Joó, G. Laurenczy, P. Karády, J. Elek, L. Nádasdi, R. Roulet, *Appl. Orgmet. Chem.* **2000**, *14*, 857-859; D. Jantke, L. Pardatscher, M. Drees, M. Cokoja, W. A. Herrmann, F. E. Kuhn, *ChemSuschem* **2016**, *9*, 2849-2854; W. Gan, D. J. M. Snelders, P. J. Dyson, G. Laurenczy, *ChemCatChem* **2013**, *5*, 1126-1132.
[16] G. Zhao, F. Joó, *Cat. Commun.* **2011**, *14*, 74-76.
[17] F. Joó, L. Nádasdi, J. Elek, G. Laurenczy, *Chem. Commun.* **1999**, 971-972; H. Horváth, G. Laurenczy, Á. Kathó, *J. Orgmet. Chem.* **2004**, *689*, 1036-1045; S. S. Bosquain, A.

Dorcier, P. J. Dyson, M. Erlandsson, L. Gonsalvi, G. Laurenczy, M. Peruzzini, *Appl. Orgmet. Chem.* **2007**, *21*, 947-951; G. Laurenczy, F. Joó, L. Nádasdi, *Inorg. Chem.* **2000**, *39*, 5083-5088; F. Joõ, *ChemCatChem* **2014**, *6*, 3306-3308; K. Sordakis, A. Guerriero, H. Bricout, M. Peruzzini, P. J. Dyson, E. Monflier, F. Hapiot, L. Gonsalvi, G. Laurenczy, *Inorg. Chim. Acta* **2015**, *431*, 132-138.

[18] A. Boddien, F. Gärtner, C. Federsel, P. Sponholz, D. Mellmann, R. Jackstell, H. Junge, M. Beller, *Angew. Chem. Int. Edit.* **2011**, *50*, 6411-6414.

[19] J. L. Drake, C. M. Manna, J. A. Byers, *Organometallics* **2013**, *32*, 6891-6894.

[20] M. Erlandsson, V. R. Landaeta, L. Gonsalvi, M. Peruzzini, A. D. Phillips, P. J. Dyson, G. Laurenczy, *Eur. J. Inorg. Chem.* **2008**, *2008*, 620-627.

[21] C. Federsel, A. Boddien, R. Jackstell, R. Jennerjahn, P. J. Dyson, R. Scopelliti, G. Laurenczy, M. Beller, *Angew. Chem. Int. Edit.* **2010**, *49*, 9777-9780; F. Bertini, I. Mellone, A. Ienco, M. Peruzzini, L. Gonsalvi, *ACS Catal.* **2015**, *5*, 1254-1265; S. Coufourier, S. Gaillard, G. Clet, C. Serre, M. Daturi, J.-L. Renaud, *Chem. Commun.* **2019**, *55*, 4977-4980.

[22] J. M. Heltzel, M. Finn, D. Ainembabazi, K. Wang, A. M. Voutchkova-Kostal, *Chem. Commun. (Camb)* **2018**, *54*, 6184-6187.

[23] G. Kovacs, G. Schubert, F. Joo, I. Papai, *Catal. Today* **2006**, *115*, 53-60.

[24] Y. Zhang, A. D. MacIntosh, J. L. Wong, E. A. Bielinski, P. G. Williard, B. Q. Mercado, N. Hazari, W. H. Bernskoetter, *Chem. Sci.* **2015**, *6*, 4291-4299.

[25] A. Azua, M. Finn, H. Yi, A. Beatriz Dantas, A. Voutchkova-Kostal, *ACS Sustain. Chem. Eng.* **2017**, *5*, 3963-3972.

[26] L. S. Sharninghausen, J. Campos, M. G. Manas, R. H. Crabtree, *Nat. Commun.* **2014**, *5*; Z. Y. Lu, I. Demianets, R. Hamze, N. J. Terrile, T. J. Williams, *ACS Catal.* **2016**, *6*, 2014-2017; Y. Li, M. Nielsen, B. Li, P. H. Dixneuf, H. Junge, M. Beller, *Green Chem.* **2015**, *17*, 193-198.

[27] L. S. Sharninghausen, B. Q. Mercado, R. H. Crabtree, N. Hazari, *Chem. Commun.* **2015**, *51*, 16201-16204.

[28] M. Pagliaro, R. Ciriminna, H. Kimura, M. Rossi, C. Della Pina, *Angew. Chem. Int. Edit.* **2007**, *46*, 4434-4440.

[29] A. Behr, J. Eilting, K. Irawadi, J. Leschinski, F. Lindner, *Green Chem.* **2008**, *10*, 13-30.

[30] M. Dusselier, P. Van Wouwe, A. Dewaele, E. Makshina, B. F. Sels, *Energ. Environ. Sci.* **2013**, *6*, 1415-1442.

[31] J. N. Starr, G. Westhoff, *Ullmann's Encycl. Ind. Chem.* **2014**, 1-8.

[32] A. Kumar, S. Semwal, J. Choudhury, *ACS Catal.* **2019**, *9*, 2164-2168.

[33] J. Su, L. Yang, X. Yang, M. Lu, B. Luo, H. Lin, *ACS Sustain. Chem. Eng.* **2015**, *3*, 195-203.

[34] A. Azua, J. A. Mata, E. Peris, F. Lamaty, J. Martinez, E. Colacino, *Organometallics* **2012**, *31*, 3911-3919.

[35] L. S. Sharninghausen, J. Campos, M. G. Manas, R. H. Crabtree, *Nat. Commun.* **2014**, *5*, 5084.

[36] U. Hintermair, U. Englert, W. Leitner, *Organometallics* **2011**, *30*, 3726-3731; A. R. Chianese, X. Li, M. C. Janzen, J. W. Faller, R. H. Crabtree, *Organometallics* **2003**, *22*, 1663-1667; G. D. Frey, C. F. Rentzsch, D. von Preysing, T. Scherg, M. Muhlhofer, E. Herdtweck, W. A. Herrmann, *J. Organomet. Chem.* **2006**, *691*, 5725-5738.

[37] M. G. Manas, J. Campos, L. S. Sharninghausen, E. Lin, R. H. Crabtree, *Green Chem.* **2015**, *17*, 594-600.

[38] A. W. Salman, R. A. Haque, S. Budagumpi, H. Zetty Zulikha, *Polyhedron* **2013**, *49*, 200-206; S. Budagumpi, R. A. Haque, A. W. Salman, M. Z. Ghdhayeb, *Inorg. Chim. Acta* **2012**, *392*, 61-72.

[39] Y. Marcus, *Chem. Rev.* **2013**, *113*, 6536-6551.

[40] S. Gülcemal , D. Gülcemal , G. F. S. Whitehead, J. Xiao, *Chem. Eur. J.* **2016**, *22*, 10513-10522.

[41] S. J. Zhang, S. D. Foyle, A. Okrut, A. Solovyov, A. Katz, B. C. Gates, D. A. Dixon, *J. Phys. Chem. A* **2017**, *121*, 5029-5044.

[42] G. P. Rosini, F. Liu, K. Krogh-Jespersen, A. S. Goldman, C. Li, S. P. Nolan, *J. Amer. Chem. Soc.* **1998**, *120*, 9256-9266.

[43] A. T. Termaten, M. Schakel, A. W. Ehlers, M. Lutz, A. L. Spek, K. Lammertsma, *Chem. Eur. J.* **2003**, *9*, 3577-3582.

[44] F. T. Ladipo, M. Kooti, J. S. Merola, *Inorg. Chem.* **1993**, *32*, 1681-1688; O. Blum, D. Milstein, *J. Amer. Chem. Soc.* **2002**, *124*, 11456-11467; D. Morales-Morales, R. Redón, Z. Wang, D. W. Lee, C. Yung, K. Magnuson, C. M. Jensen, *Can. J. Chem.* **2001**, *79*, 823-829.

[45] V. Guiral, F. Delbecq, P. Sautet, *Organometallics* **2000**, *19*, 1589-1598; S. M. Ng, C. Zhao, Z. Lin, *J. Organomet. Chem.* **2002**, *662*, 120-129; H. Itagaki, N. Koga, K. Morokuma, Y. Saito, *Organometallics* **1993**, *12*, 1648-1654; M. Yamakawa, H. Ito, R. Noyori, *J. Amer. Chem. Soc.* **2000**, *122*, 1466-1478.

[46] G. Kovács, G. Schubert, F. Joó, I. Pápai, *Catal. Today* **2006**, *115*, 53-60.

[47] Y.-y. Ohnishi, T. Matsunaga, Y. Nakao, H. Sato, S. Sakaki, *J. Amer. Chem. Soc.* **2005**, *127*, 4021-4032.

[48] L. S. Sharninghausen, R. H. Crabtree, *Isr. J. Chem.* **2017**, *10.1002/ijch.201700048*.

[49] D. Jantke, M. Cokoja, A. Pöthig, W. A. Herrmann, F. E. Kühn, *Organometallics* **2013**, *32*, 741-744; A. Azua, S. Sanz, E. Peris, *Chem. Eur. J.* **2011**, *17*, 3963-3967; D. Jantke, L. Pardatscher, M. Drees, M. Cokoja, W. A. Herrmann, F. E. Kühn, *ChemSusChem* **2016**, *9*, 2849-2854.

[50] C. F. Rentzsch, E. Tosh, W. A. Herrmann, F. E. Kuhn, *Green Chem.* **2009**, *11*, 1610-1617; M. V. Jiménez, J. Fernández-Tornos, J. J. Pérez-Torrente, F. J. Modrego, P. Garćia-Orduña, L. A. Oro, *Organometallics* **2015**, *34*, 926-940.

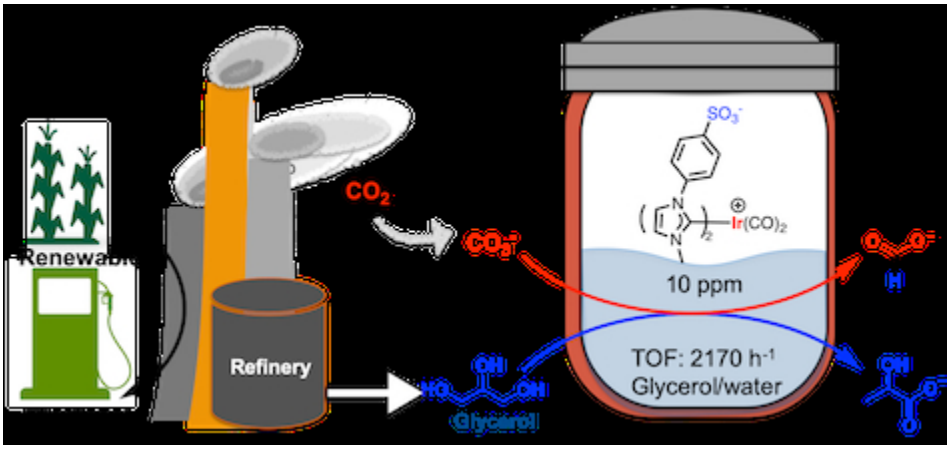
Renewable
Refinery
CO_2
CO_2
SO_3^-
$Ir(CO)_2$
10 ppm
TOF: 2170 h^{-1}
Glycerol/water
Glycerol
H